Experimental Mechanics
https://doi.org/10.1007/s11340-018-0426-z

BRIEF TECHNICAL NOTE

Measurement of a Nearly Friction-Free Stress–Strain Curve of Silicone Rubber up to a Large Strain in Compression Testing

Sanghoon Kim [1] · Minkyu Kim [1] · Hyunho Shin [2] · Kyong-Yop Rhee [1]

Received: 3 March 2018 / Accepted: 20 August 2018

Abstract
Nominal stress–strain curves of a silicone rubber specimen with a range of length-to-diameter (L/D) ratios have been measured via compression testing. The curves are highly dependent on the L/D ratio. The contact area has been measured using stamp ink applied to the sidewall of the specimen to determine the optimal L/D ratio which yields the stress–strain curve closest to the curve of the friction-free specimen. Traces of ink appear on the platen after the compression test, indicating that the phenomenon of rollover takes place. When the L/D ratio is less than 1.0, the contact area is less than that of the friction-free specimen although the phenomenon of rollover supplements the contact area. When the L/D ratio increases up to 1.0, the contact area increases toward that of the ideal specimen that deforms uniformly under the friction-free condition; the stress–strain curve of the specimen with the L/D ratio of 1.0 can be regarded as the nearly friction-free property of silicone rubber.

Keywords Nearly friction-free property · Stress–strain curve · Uniaxial compression · Silicone rubber · Rollover of the side wall

Introduction

A reliable constitutive model and its precise calibration are two prerequisites to an accurate computer simulation of the mechanical deformation of materials and structures [1, 2]. Rubber is often subjected to compressive loading up to a large strain (e.g., up to the nominal strain of even 90%). For the simulation of such compressive deformation of rubber, it is desirable to calibrate a constitutive model using a compressive stress–strain curve constructed up to a large strain [3–9].

A stress–strain curve measured under a friction-free condition is required to calibrate a constitutive model. Otherwise, the obtained stress–strain curve is not the true material property but merely a load-displacement indicator of a compression event in the testing machine that takes place under the influence of friction; the specimen deforms non-uniformly in shape and is no longer in the uniaxial and homogeneous stress state. However, determining the friction-free stress–strain curve of materials under uniaxial compression is not a simple task. For a plastically deforming metallic material (the Poisson's ratio is approximately 0.5), barreling and rollover (non-uniform deformation) of the specimen usually take place because of friction, indicating an inhomogeneous and non-uniaxial stress state. The phenomena of barreling and rollover lead to overestimation of the stress–strain curve [10–17]. Such an influence of friction increases as the length-to-diameter (L/D) ratio of the specimen decreases. Therefore, the use of a specimen with a higher L/D ratio (generally about 2) is desirable for metallic materials, provided that the phenomenon of buckling can be avoided.

Elastically deforming rubber (a Poisson's ratio of approximately 0.5) will produce larger amounts of friction than metallic materials, resulting in a greater amount of barreling and rollover [9]. The resulting stress–strain curve for elastically deforming rubber is likely overestimated because of the increased friction; the stress–strain curves of rubber are also different notably depending on the L/D ratio. Such a result imposes a difficulty in selecting a curve to be used for the

✉ Hyunho Shin
hshin@gwnu.ac.kr

✉ Kyong-Yop Rhee
rheeky@khu.ac.kr

1 Mechanics of Nano-composites and Design Laboratory, Department of Mechanical Engineering, Kyunghee University, 1732 Dukyoungdae-ro, Yongin, Gyeonggi-do 17104, Republic of Korea

2 Mechanics of Materials and Design Laboratory, Department of Materials Engineering, Gangneung-Wonju National University, 7 Jugheon-ghil, Gangneung, Gangwon-do 25457, Republic of Korea

Published online: 24 September 2018

calibration of a constitutive model as the friction-free curve. Although there has been considerable interest in measuring the compressive stress–strain curve of rubber [3–9], it is not easy to find studies that aimed to obtain the friction-free property, probably because an appropriate methodology was unavailable. In this regard, the necessity of developing a method for measuring the friction-free stress–strain curve is high.

This study sets up a *procedure* for measuring the nearly friction-free stress–strain curve of rubber as follows. If one can measure the current contact area of rubber with the platens simultaneously with the measurement of the compressive stress–strain curve, the curve of the current contact area of the real specimen can be compared with that of the ideal specimen that deforms in the friction-free state; the current contact area of the ideal (friction-free) specimen can be calculated suitably by considering the volume constancy of an incompressible solid (a Poisson's ratio of approximately 0.5): $A_c L_c = A_o L_o$, where A and L are cross-sectional area and length, respectively, and the subscripts c and o denote the current and initial values, respectively. If the current contact areas of a series of specimens having a range of L/D ratios are compared with that (A_c) of the ideal specimen, it is postulated that the desirable (optimal) L/D ratio that results in the closest current contact area to that of the ideal specimen can be determined. The stress–strain curve measured at the optimal L/D ratio is closest to the friction-free stress–strain curve; it can be regarded as a nearly friction-free stress–strain curve.

The current contact area of rubber can be measured during the compression test using an appropriate apparatus based on various techniques, such as digital image correlation and 3D position measurement. This study introduces an alternative *method* for measuring the current contact area as follows. If we apply stamp ink onto the sidewall of the specimen at the beginning of the compression test, it is hypothesized that traces of ink will be left on the platen after the tests to allow measurement of the contact area and identification of the rollover-induced area. This method of measuring the current contact area is easy to carry out (handy) and economical. Its efficiency is to be tested in this study.

Once the above *procedure* and *method* for measuring the contact area are experimentally demonstrated, they may be useful for measuring nearly friction-free compressive stress–strain curves of various types of rubber material. The purpose of this study is to demonstrate that a nearly friction-free stress–strain curve of silicone rubber can be obtained successfully up to a fairly large compressive strain (a nominal strain of 0.9) using the above procedure and method.

Experimental Procedure

Commercial silicone rubber pads with varying thicknesses were machined to fabricate cylinder (disk) specimens. The diameter of the specimens was constant (10 mm), resulting in specimens with a range of L/D ratios: 0.1, 0.2, 0.4, 0.8, and 1.0.

Compression testing was carried out using a universal tester (Model 3367, Instron, Buckinghamshire, UK). An aliquot of lubricant (silicone oil) was applied to the contact area between the specimen and the top/bottom platen made of stainless steel. The load applied on the specimen was measured using a 30-kN load cell. The axial displacement of the specimen was determined by measuring the relative distance of the top/bottom platen using a contact-type spring-back displacement sensor (Model KTR2-10 mm, Miran Tech. Co. Ltd., Shenzen, China). The nominal stress of the specimen (σ_n) was determined based on the equation $\sigma_n = F/A_o$, where F is the current load measured using the load cell, and A_o is the initial cross-sectional area of the specimen. The nominal strain of the specimen (ε_n) was determined based on the relationship $\varepsilon_n = (l_c - l_o)/l_o$, where l_c and l_o are the current and initial lengths of the specimen, respectively. The true stress of the specimen (σ_t) was determined using the relationship $\sigma_t = F/A_c$, where A_c is the current cross-sectional area of the specimen. The true strain (ε_t) of the specimen was determined using the equation $\varepsilon_t = \ln(l_c/l_o)$. Tests for the series of specimens with a range of L/D ratios were carried out at a nominal strain rate ($\dot{\varepsilon}_n$) of 10^{-3} s^{-1}. Once the desirable (optimal) L/D ratio (1.0 for silicone rubber, as will be shown later in this study) was determined based on the measured current contact area, additional tests at nominal strain rates of 10^{-2} and 10^{-4} s^{-1} were carried out for specimens with the optimum L/D value (=1.0). The speed of the cross head (dL/dt) was constant, and its value at a given nominal strain rate ($\dot{\varepsilon}_n$) was determined using the relationship $dL/dt = L_o\dot{\varepsilon}_n$. All tests were carried out at ambient temperature.

At the beginning of the compression test, stamp ink (purchased at a local stationary store) was applied to the sidewall of the specimen. After the test, the image of the ring-type ink mark that appeared on the steel platen was photographed (Examples of the ring-type mark will be presented later in Fig. 2.). The average value of the outer diameter of the ring mark was quantified using image-processing software (Image J). For this purpose, first, information on the number of pixels per centimeter (N_c) was obtained from the image of the ruler included in the same photograph. Second, three diagonal lines were artificially drawn on the image of the ring mark, resulting in six contact points (60° apart) between the diagonal lines and outer periphery of the ring mark. Third, the number of pixels (N) between the contact points on a given diagonal line was counted using Image J. Finally, the diameter of the ring mark

(d) was determined using the relationship $d = N/N_c$. For each ring mark, the diameter was determined in this way three times using the three diagonal lines; the areas of the ring mark calculated from the three diameter values were averaged.

Results and Discussion

The nominal stress–strain curves were highly dependent on the L/D ratio, as shown in Fig. 1. This L/D-ratio dependency results from the influence of friction between the specimen and platen; the influence of friction increases with the decrease of the L/D ratio [10–17].

The stress–strain curves in Fig. 1 initially shift downward as the L/D ratio increases, similar to the behavior of metallic specimens [10–17]. However, the stress–strain curve shifts upward as the L/D ratio increases for nominal strains above approximately 0.87. In other words, in the large nominal strain regime, the specimen with a higher L/D ratio, at first look, seems to overestimate the stress–strain curve. This behavior is contrary to the case when the nominal strain is less than approximately 0.87.

In this study, the specimen that deforms uniformly without volume change in the friction-free state is named the ideal specimen (or the friction-free specimen). The stress–strain curve of the ideal specimen is called the friction-free stress–strain curve. From the findings in Fig. 1 (described in the above paragraph), it is difficult to select the stress–strain curve that is closest to the friction-free stress–strain curve of silicone rubber. The ink mark remaining on the steel platen after the compression test was measured to examine the observed stress–strain behavior. Examples of the ink mark remaining on the surface of the stainless-steel platen are illustrated in Fig. 2. The stamp ink was only applied to the sidewall of the specimen, so any trace of ink on the platen would be direct evidence of rollover of the sidewall caused by high-friction barreling.

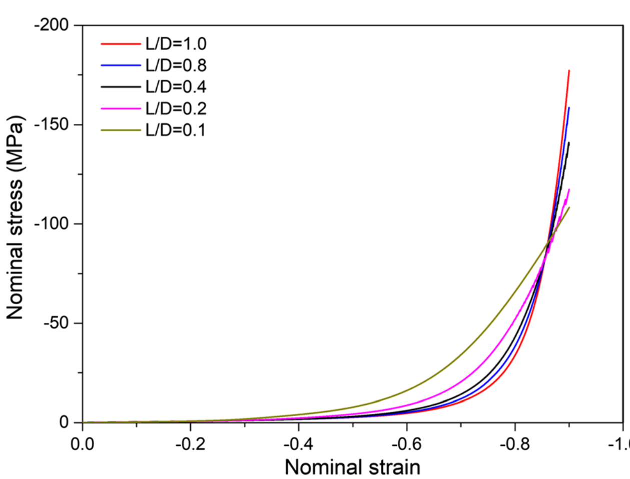

Fig. 1 Nominal stress–strain curves of specimens with varying L/D ratios

To analyze the ink mark on the steel platen, in Fig. 2(e), the concepts of the radially expanded version of the initial contact area (noted as region 1), the rollover induced contact area (region 2), and the total contact area (region 3, which is region 1 plus region 2) are schematically drawn. During unloading, the rubber material in region 2 was observed to shift mainly along direction 2, as indicated in Fig. 2(f); no appreciable inward drag of ink was observed at the outer periphery of the ring mark (noted as M in Fig. 2). Therefore, the diameter of ring M in Fig. 2 is the direct indicator of the total contact area of the specimen.

The initial contact area of the specimen expands radially as the compression test proceeds. Because stamp ink was not applied onto the initial contact area, the inner un-marked portion of the ink traces shown in Fig. 2 should be associated with region 1 (the radially expanded version of the initial contact area). However, the outer periphery of region 1 is not clear in Fig. 2, because ink located at the outer periphery of region 1 during unloading is pulled inward with radial shrinkage of the specimen along direction 1 (Fig. 2(f)). Therefore, it is difficult to quantify the area of region 1 from the ink traces without ambiguity.

From the above findings, this study quantified only the total contact area. The averaged total contact area quantified by the method described in "Experimental Procedure" section is presented in Fig. 3 as a function of the nominal strain. Included in Fig. 3 is the ideal current contact area of the friction-free specimen (A_c), that was calculated from the initial area of the specimen (A_o) based on the assumption of the volume constancy condition in the friction-free state: $A_cL_c = A_oL_o$.

The total contact area, including the rollover-induced contact area, was less than the ideal contact area for L/D ratios less than 1.0, as shown in Fig. 3. The total contact area of the specimen was reasonably consistent with the contact area of the ideal (friction-free) specimen for an L/D ratio of 1. Therefore, the stress–strain curve of this specimen (L/D = 1.0) is closest to the friction-free stress–strain curve among the curves presented in Fig. 1.

After the optimal L/D ratio of 1.0 was determined at a nominal strain rate of 10^{-3} s^{-1}, additional tests were carried out at 10^{-2} and 10^{-4} s^{-1} to check whether the measured contact area is independent of the strain rate. The results are included in Fig. 3. Figure 3 shows that the measured contact areas at the nominal strain rates of 10^{-2} and 10^{-4} s^{-1} are reasonably consistent with that at 10^{-3} s^{-1}. This finding indicates that the *speed* of rollover of the side wall (where ink was applied) does not influence the *size* of the ring mark that forms during loading. During unloading, as mentioned, movement of region 2 does not influence the size of the already-formed ring

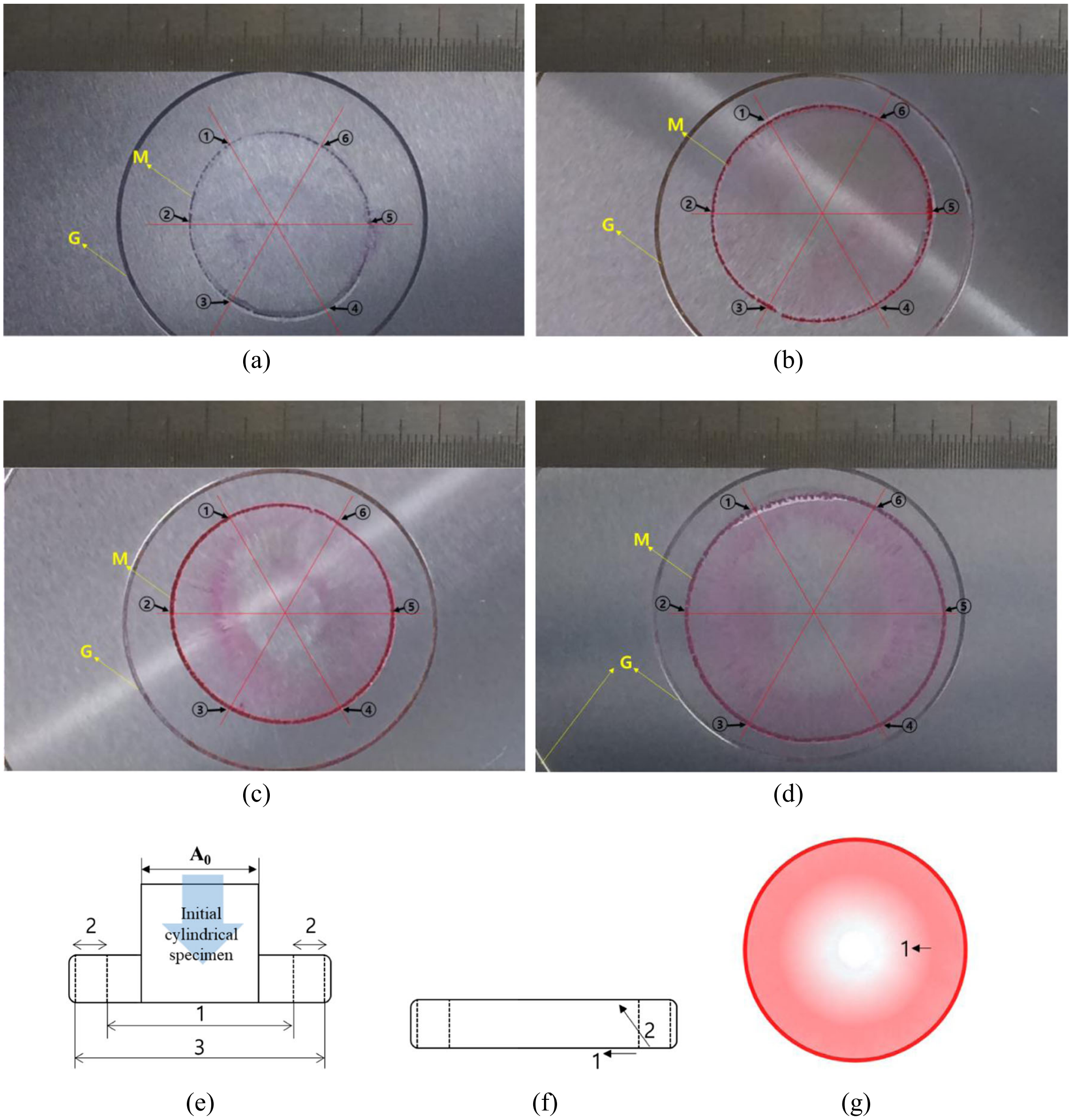

Fig. 2 Examples of the ink mark remaining on the surface of the stainless-steel platen after the compression test up to a nominal strain of 0.9. (**a**) L/D = 0.2, (b) L/D = 0.4, (**c**) L/D = 0.8, and (**d**) L/D = 1.0. M: outer periphery of the ink mark. G: grooved ring on the steel platen. Cross lines at 60° interval were drawn to find contact points (marked as circled numbers) for measurement of the diameter in image processing software. (**e**) Schematic illustration of the concept of the contact area. 1: Radially expanded version of the initial contact area, 2: the rollover-induced contact area, and 3: the total contact area. (**f**) Directions of the movement of the material during unloading. Arrow 1 indicates the shrinkage direction of the material at the outer periphery of region 1 and arrow 2 indicates that in region 2. (**g**) Schematic illustration of the in-plane (radial) shrinkage of the outer edge of region 1 that results in the inward drag of ink due to physical bonding

mark. Therefore, the method for measuring the total contact area using stamp ink can be used in quasi-static tests in a wide range of strain rates (at least up to a strain rate of 10^{-2} s^{-1}). No reason can be found why formation of the outer periphery should be influenced by a slower strain rate than 10^{-4} s^{-1}; there seems to be no lower limit of the strain rate for use of stamp ink. As for the maximum limit of the strain rate up to which the current method can be applied, further study is needed.

The nominal stress–strain curve of the specimen with an L/D ratio of 1.0 (Fig. 1) was converted to the true stress–strain curve by assuming that the specimen is ideal (friction free), as shown by the solid curve (red) in Fig. 4. The dashed curve (red) of Fig. 4 was constructed based on the measured contact area (the dashed curve in Fig. 3(d)). The two red curves for the specimen with L/D = 1.0 are reasonably consistent up to the measured strain, which indicates that the nominal stress–strain curve of this specimen (Fig. 1) and the true stress–strain curve

Fig. 3 Comparison of the measured total contact area (dashed curves with data points) with the ideal contact area (solid curves) for the case when the L/D ratio is (**a**) 0.2, (**b**) 0.4, (**c**) 0.8, and (**d**) 1.0. The dashed curves were constructed using measured data points based on the Levenberg-Marquardt algorithm implemented in commercial software (OriginLab)

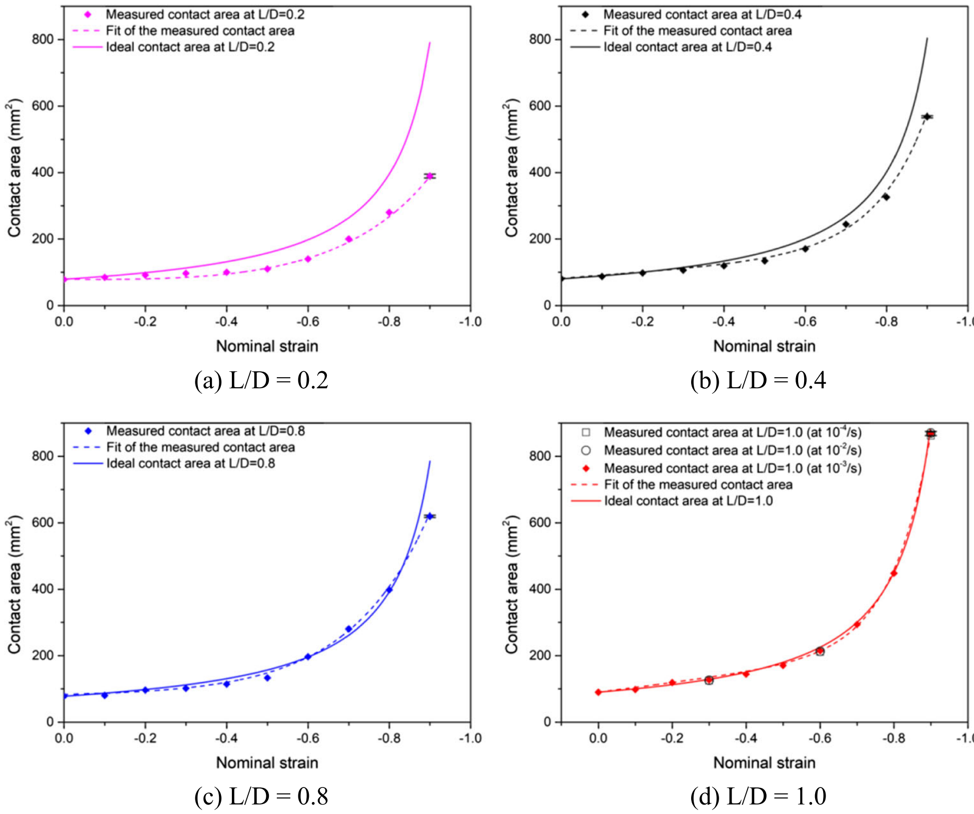

(shown as a dashed curve in red in Fig. 4) are close to the friction-free curve.

Examples of stress–strain curves of specimens with inappropriate L/D ratios (purple for L/D = 0.2, black for L/D = 0.4, and blue for L/D = 0.8) are also included in Fig. 4. The difference between the solid and dashed curves for L/D < 1 in Fig. 4 indicate that these curves are not friction-free ones.

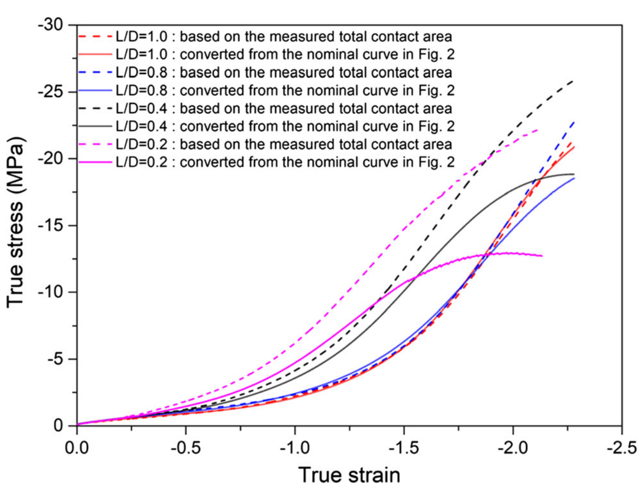

Fig. 4 True stress–strain curves (solid curves) converted from the nominal curves in Fig. 1 by assuming that the specimen is ideal. Dashed curves were constructed based on the measured total contact area (dashed curves in Fig. 3)

The rollover of the specimen is the result of significant barreling and is believed to diminish the degree of barreling. However, the specimen was still slightly barreling even after rollover occurred, as schematically illustrated in Fig. 2(f). The specimen with an L/D ratio of 1.0 had practically the same contact area as the ideal specimen, even with a slight (residual) barelling. The stress–strain curve may still slightly overestimate the material behavior, indicating a nonuniaxial and inhomogeneous stress state in the specimen. For this reason, the curve of the specimen with an L/D ratio of 1.0 is called the nearly friction-free stress–strain curve instead of the perfectly friction-free one. However, the selected stress–strain curve, from the viewpoint of the total contact area, is closest to the friction-free stress–strain curve of silicone rubber among the experimentally determined curves presented in Fig. 1.

The results in this study may be useful for future studies aiming at measuring friction-free compressive stress–strain curves of various types of rubber material; the followings are tips (recommendations) for such future studies. For other types of rubber materials, there is no guarantee that the proximity of the measured contact area to the friction-free contact area is achieved at the L/D ratio of 1.0. However, according to the result of this study, it may be desirable to test the given rubber material at the L/D ratio of 1.0 *first* to reduce the number of tests. It is cautiously anticipated that the optimal value of the L/D ratio of a rubber material may not be far away from the value of 1.0.

For the case of silicone rubber used in this study, the maximum strain, up to which the proximity of the area curves is achieved, increases as the L/D ratio increases (see Fig. 3). Figure 3 shows that it is difficult to achieve the proximity at a nominal strain of 0.9, which is the maximum strain limit tested in this study. Therefore, if the proximity is achieved at the nominal strain of 0.9, the proximity in the smaller strain regime is guaranteed.

This study presented a *procedure* for measuring the friction-free compressive stress–strain curve by comparing the measured current contact area with the ideal (friction-free) contact area calculated from the condition of volume constancy of the friction-free specimen. It also presented a handy *method* to quantify the total contact area. The application of stamp ink to the sidewall of a rubber specimen appears to be an efficient method to quantify the current contact area and is informative for selecting the L/D ratio of the specimen from the viewpoint of the proximity of the area curve of the current specimen to the ideal specimen. It was demonstrated that a nearly friction-free stress–strain curve of silicone rubber can be obtained successfully up to a fairly large compressive strain (up to the nominal strain of 0.9) using the presented procedure and method.

Acknowledgements This study was financially supported by the Basic Science Research Program under contract numbers 2017R1A6A3A11028683 (S. Kim) and 2015R1A2A2A01002454 (H. Shin) through a National Research Foundation (NRF) grant funded by the Ministry of Education (Korea).

References

1. Ju ML, Jmal H, Dupuis R, Aubry E (2015) Visco-hyperelastic constitutive model for modeling the quasi-static behavior of polyurethane foam in large deformation. Polym Eng Sci 55:1795–1804
2. Kim W-D, Kim W-S, Woo C-S, Lee H-J (2004) Some considerations on mechanical testing methods of rubbery materials using nonlinear finite element analysis. Polym Int 53:850–856
3. Gent AN, Discenzo FM, Suh JB (2009) Compression of rubber disks between frictional surfaces. Rubber Chem Technol 82:1–17
4. Bradley GL, Chang PC, Mckenna GB (2001) Rubber modeling using uniaxial test data. J Appl Polym Sci 81:837–848
5. Williams JG, Gamonpilas C (2008) Using the simple compression test to determine Young's modulus, Poisson's ratio and the coulomb friction coefficient. Int J Solids Struct 45:4448–4459
6. Doman DA, Cronin DS, Salisbury CP (2006) Characterization of polyurethane rubber at high deformation rates. Exp Mech 46:367–376
7. Dar UA, Zhang W, Xu Y, Wang J (2014) Thermal and strain rate sensitive compressive behavior of polycarbonate polymer-experimental and constitutive analysis. J Polym Res 21:519
8. Mansouri MR, Darijani H, Baghani M (2017) On the correlation of FEM and experiments for hyperelastic elastomers. Exp Mech 57:195–206
9. Mesa-Múnera E, Ramírez -Salazar JF, Boulanger P, Branch JW (2012) Inverse-FEM characterization of a brain tissue phantom to simulate compression and indentation. Ing y Cienc 8:11–36
10. Schroeder W, Webster DA (1949) Press-forging thin sections-effect of friction, area, and thickness on pressures required. J Appl Mech ASME 16:289–294
11. Hill R (1998) The mathematical theory of plasticity. Oxford University Press Inc., New York
12. Rand JL (1967) An analysis of the split Hopkinson pressure bar. NOLTR 67–156, White Oak
13. Cha SH, Shin H, Kim JB (2010) Numerical investigation of frictional effects and compensation of frictional effects in split hopkinson pressure bar (SHPB) test. Trans Korean Soc Mech Eng A 34:511–518
14. Banerjee JK (1985) Barreling of solid cylinders under axial compression. J Eng Mater Technol 107:138–144
15. Christiansen P, Martins PAF, Bay N (2016) Friction compensation in the upsetting of cylindrical test specimens. Exp Mech 56:1271–1279
16. Khan AS, Balzer JE, Wilgeroth JM, Proud WG (2014) Aspect ratio compression effects on metals and polymers. J Phys Conf Ser 500
17. Espinosa HD, Patanella A, Fischer M (2000) A novel dynamic friction experiment using a modified Kolsky bar apparatus. Exp Mech 40:138–153